Available online at www.sciencedirect.com

ScienceDirect

Ceramics International 39 (2013) 8581–8588

CERAMICS INTERNATIONAL

www.elsevier.com/locate/ceramint

Phase-formation, microstructure, and piezoelectric/dielectric properties of $BiYO_3$-doped $Pb(Zr_{0.53}Ti_{0.47})O_3$ for piezoelectric energy harvesting devices

Man-Soon Yoon, Iqbal Mahmud, Soon-Chul Ur*

Department of Materials Science and Engineering/RIC-ReSEM, Korea National University of Transportation, 50 Daehangno, Chungju, Chungbuk 380-702, Republic of Korea

Received 12 February 2013; received in revised form 2 April 2013; accepted 10 April 2013
Available online 18 April 2013

Abstract

This paper proposes a method for the composition and synthesis of lead zirconate titanate (PZT) piezoelectric ceramic for use in energy harvesting systems. The proposed material consists of $(1-x)Pb(Zr_{0.53}Ti_{0.47})O_3$–$xBiYO_3$ [PZT–BY(x)] ($x=0$, 0.01, 0.02, 0.03, 0.04, and 0.05 mol) ceramics near the morphotropic phase boundary (MPB) region, prepared by a solid-state mixed-oxide method. The optimum sintering temperature was found to be 1160 °C, which produced high relative density for all specimens (96% of the theoretical density). Second phases were found to precipitate in the composition containing $x\geq0.01$ mol of BY. It is shown that the addition of BY inhibits grain growth, and exhibits a denser and finer microstructure than those in the un-doped state. Fracture surface observation revealed predominant intergranular fracture for $x=0$ and $x=0.01$, while a mixed mode of transgranular and intergranular fracture appeared for $x\geq0.02$. The optimal doping level was found to be $x=0.01$, for which a dielectric constant (K_{33}^T) of 750, a Curie temperature (T_C) of 373 °C, a remnant polarization (P_r) of 50 μC/cm^2, a piezoelectric constant (d_{33}) of 350 pC/N, and an electro-mechanical coupling factor (k_p) of 65% were obtained. In addition, the piezoelectric voltage constant (g_{33}), and transduction coefficient ($d_{33}\times g_{33}$) of PZT–BY(x) ceramics have been calculated. The ceramic PZT–BY(0.01) shows a considerably lower K_{33}^T value, but higher d_{33} and k_p. Therefore, the maximum transduction coefficient ($d_{33}\times g_{33}$) of 18,549 × 10^{-15} m^2/N was obtained for PZT–BY(0.01). The large ($d_{33}\times g_{33}$) indicates that the PZT–BY(0.01) ceramic is a good candidate material for energy harvesting devices.

Keywords: A. Sintering; B. Grain size; D. PZT; Energy harvesting

1. Introduction

Recently, energy harvesting from vibration and motion sources has attracted much interest, particularly for micro power sources [1,2]. To convert this mechanical energy to electrical energy, vibration energy harvesters use one of three methods: electrostatic induction, electromagnetic induction, and the piezoelectric effect [3,4]. Among these transducers, piezoelectric harvesters are preferred due to their simplicity, easy maintenance, and durability. Depending on the given application, high power density is required in piezoelectric technology, for which a large electro-mechanical coupling effect is required [5,6]. In addition, systems should be much simpler, without external voltage sources. Lead zirconate titanate (PZT) has relevant piezoelectric properties, and is usually used as an energy conversion material in piezoelectric structures. Numerous relevant studies on piezoelectric harvesters have been performed in the last decade [7–10]. Suitable piezoelectric materials for vibration energy conversion to electrical energy are characterized by a large magnitude of the product of the piezoelectric voltage constant (g_{33}) and the piezoelectric charge constant (d_{33}), which is called the transduction coefficient ($d_{33}\times g_{33}$) [11–13]. Recently, many studies have been conducted to find such piezoelectric materials [11–14]. According to the definition of g_{33} expressed by $d_{33}/(\varepsilon_0\times K_{33}^T)$ (where K_{33}^T is the dielectric constant and ε_0 is dielectric permittivity of free space), a high energy density could be obtained from piezoelectric materials with a large d_{33} value and small K_{33}^T. A higher product of d_{33} and g_{33}, i.e., a higher figure of merit ($d_{33}\times g_{33}$), can provide higher energy output, and hence, the value is an essential criterion for energy

*Corresponding author. Tel.: +82 43 841 5385; fax: +82 43 841 5380.
E-mail addresses: scur@ut.ac.kr, urwin@hanmail.net (C. Ur).

0272-8842/$ - see front matter © 2013 Elsevier Ltd and Techna Group S.r.l. All rights reserved.
http://dx.doi.org/10.1016/j.ceramint.2013.04.031

harvesting materials [15,16]. Many investigations have been conducted to obtain piezoelectric ceramics with a high d_{33} value and small K_{33}^{T} [17–19].

From considerations of ionic radii, it is probable that bismuth (Bi) and yttria (Y) ions occupy the Pb site, and that charge compensation will take place by the creation of Pb vacancies in the lattice, which facilitate the movement of the domain wall so as to improve the piezoelectric and dielectric properties [20–25]. It was reported that the substitution of Bi in PZT increased sinterability, retarded grain growth, and decreased grain size [22–24]. In addition, it was also reported that a uniform grain size distribution with decreasing grain size yielded a large P_r and a small leakage current in Y-doped PZT materials [20,21,25]. Bi and/or Y doping in PZT would be expected to increase d_{33} and K_{33}^{T} but decrease the g_{33} value. Since $BiYO_3$ (BY) generally shows a low dielectric constant, one can predict that pre-synthesized BY can act as a dopant to reduce the dielectric constant in PZT. A preliminary study indicated that pre-synthesized BY doped into PZT could remain as a precipitate after sintering, according to X-ray diffraction analysis. This implies that BY can act as a grain growth inhibitor and as donors in the vicinity of grains. Thus, the existence of BY precipitate can have an influence on the grain growth and the piezoelectric and dielectric properties, in contrast to direct doping methods.

The main purpose of the present study is to demonstrate the possibility of optimum energy harvesting material with a high figure of merit ($d_{33} \times g_{33}$) by controlling the pre-synthesized BY contents. To this end, we investigate the effect of pre-synthesized BY content on the crystal structure and microstructure, and analyze the piezoelectric/dielectric properties in the PZT–BY system to search for the optimum compositions with high d_{33} and low K_{33}^{T}.

2. Experimental procedure

A conventional mixed oxide method was used to fabricate $(1-x)Pb(Zr_{0.53}Ti_{0.47})O_3$–$xBiYO_3$ (abbreviated as PZT–BY(x) hereafter) containing various amounts of BY ($0 \le x \le 0.05$). To eliminate the effects associated with the direct co-doping of Bi_2O_3 and Y_2O_3, a pre-synthesis method was used for the fabrication of PZT–BY(x) by a ball mill process. The first stage of the fabrication was the synthesis of PZT and BY. A stoichiometric amount of analytical-reagent (AR)-grade PbO (99.5%, Dansuk, Korea), ZrO_2 (99.5%, Daichi, Japan), and TiO_2 (99.9%, High purity Chemicals, Japan) to synthesize PZT; and Bi_2O_3 (99.9%, High purity Chemicals, Japan) and Y_2O_3 (99.9%, High purity Chemicals, Japan) to synthesize BY were weighed and then ball milled in distilled water using ZrO_2 media for 24 h. The dried powders were discretely sieved through 100 mesh and separately calcined at 850 °C for 2 h in alumina crucibles. X-ray analysis at this stage indicated a single phase. The second stage the PZT–BY(x) was fabricated by first weighing the pre-synthesized PZT and BY powders and ball-milling them for 72 h. The dried powders were pressed into a 15-mm-diameter disk and then subjected to cold isostatic pressing (CIP) under a pressure of 147.2 MPa. The pressed pellets were sintered at various temperatures. To limit PbO loss from pellets, a PbO-rich atmosphere was maintained by placing an equimolar mixture of PbO and ZrO_2 inside a covered alumina crucible. The sintered specimens were then ground to maintain the required aspect ratio (diameter/thickness ≥15) with an average diameter of 11.7 mm and thickness of 0.75 mm for measuring the radial vibration mode of the piezoelectric properties. In addition to this, a cube sample with an edge length of 10 mm was also prepared to measure the d_{31} value following measuring instruction of a d_{33}/d_{31} meter (IACAS; Model ZJ-6B) at the optimum composition.

A preliminary study on the dielectric/piezoelectric properties of the PZT–BY(x) system indicated that the 0.99Pb$(Zr_{0.53}Ti_{0.47})O_3$–$0.01BiYO_3$ composition had excellent dielectric/piezoelectric properties. Thus, specimens with the same composition were prepared by conventional mixed-oxide method without a pre-synthesizing process to investigate the processing effects. A stoichiometric amount of the AR-grade powders were simultaneously mixed and dried. The dried powder was calcined at 850 °C for 2 h.

The specimens were characterized by X-ray diffractometer (XRD, Rigaku D/Max-2500H, Japan) with Cu Kα radiation after calcination and sintering. The morphologies and microstructures of all of the powders and sintered samples were investigated using a scanning electron microscope (SEM; Hitachi S-2400). In order to measure the electrical properties, silver paste was coated to form electrodes on both sides of the sample, and then subsequently fired at 560 °C for 30 min. To investigate the proper poling conditions, each specimen was poled in stirred silicon oil at 120 °C, by applying a DC electric field of 4–8 kV/mm for 45 min, and subsequent aging at 120 °C for 3 h. Preliminary study indicated that the spontaneous polarization was not fully saturated under a DC electric field of 4 kV/mm. The dielectric and the piezoelectric properties of the aged samples were then measured and evaluated. Based on these results, the optimum poling voltage chosen as 4.0 kV/mm. Considering the fact that deviations of the electric properties could exist in the measured samples, five specimens were prepared and tested for each batch. The piezoelectric coefficient was determined using a d_{33}/d_{31} meter (IACAS; Model ZJ-6B), and the electromechanical and dielectric properties were calculated by a resonance/anti-resonance measurement method [26] using an impedance/gain phase analyzer (HP-4194A). The temperature dependence of the dielectric constant and the dissipation factor over a range of −25 to 500 °C was measured using an automated system at 1 kHz, in which an HP-4194A Impedance/Gain-Phase Analyzer and a temperature-control box (−40 to 150 °C: Delta 9023 chamber, 150–500 °C: Lindberg tube furnace) were controlled by a computer system. The temperature was measured using a Keithley 740 thermometer with a K-type thermocouple mounted on the samples. The behavior of the polarization electric field was determined using a Precision LC system (Radiant Technology Model: 610E).

3. Results and discussions

3.1. Effects of pre-synthesized $BiYO_3$ doping on the crystal structure and microstructure

Fig. 1 shows the XRD patterns for the calcined BY and PZT. A full stabilization of the cubic phase was achieved for the BY (JCPDS no. 271047), as shown in Fig. 1(a). In

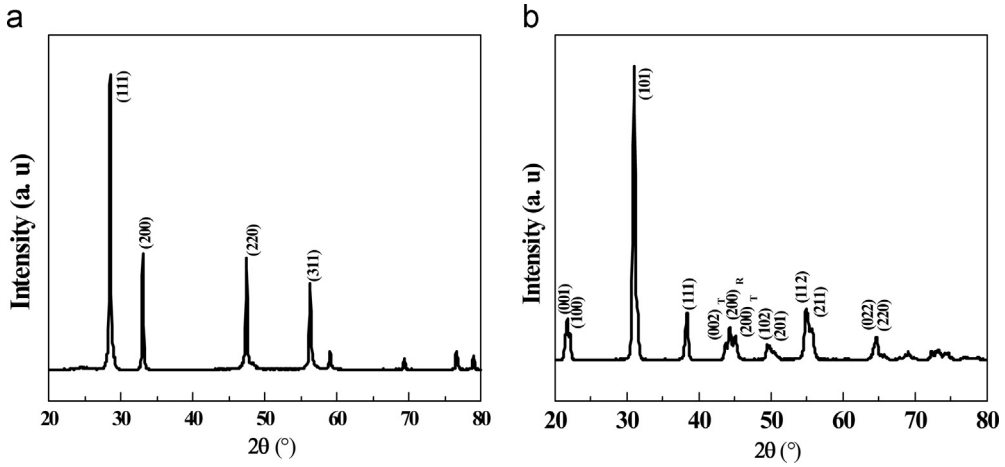

Fig. 1. XRD patterns of (a) $BiYO_3$ (b) $Pb(Zr_{0.53}Ti_{0.47})O_3$ powder calcined at 850 °C for 2 h.

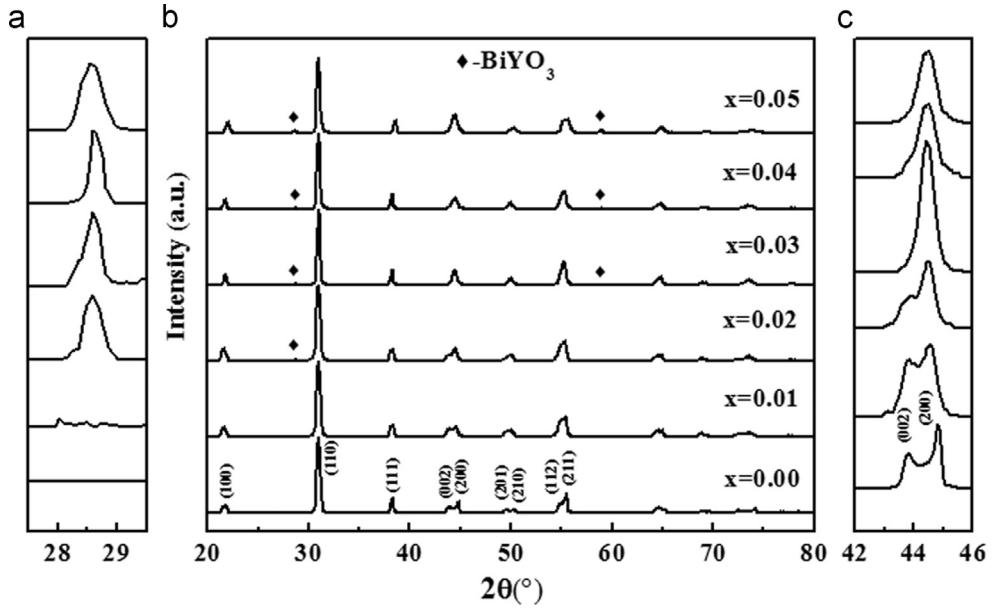

Fig. 2. (a) XRD multi plot patterns of PZT–BY(x) ($0 \le x \le 0.05$) system sintered at 1160 °C for 2 h, (b) and (c) enlarged portion of XRD at selected 2θ angle [♦ indicates the second phase].

addition, the calcined PZT powder was also fully stabilized to the perovskite structure (JCPDS no. 01-070-4264) without any second and/or pyrochlore phases. The pure PZT shows the coexistence of tetragonal and rhombohedral symmetry. Fig. 2 shows the X-ray diffraction patterns for the sintered PZT−BY (x) samples fabricated through a pre-synthesis process. All of them were sintered at 1160 °C for 2 h. As shown in Fig. 2(a), two compositions ($x=0$, 0.01) are fully stabilized to the perovskite structure. The enlarged XRD patterns of the ceramics in the 2θ range of 42–46° [Fig. 2(c)] indicate that the (002) peak is suppressed and the rhombohedral phase increases with an increasing amount of BY. It is also shown that tetragonality decreases with increasing BY content. This in turn means that the PZT–BY(0.01) composition shows the MPB. Furthermore, a second peak appeared as the BY addition was increased to more than 0.01 mol, suggesting the precipitation of BY [Fig. 2(b)].

The microstructures of the sintered samples were observed by SEM, and the fracture surface micrographs for samples containing various amounts of BY are shown in Fig. 3(a)–(f). It is evident that the addition of BY brings about a significant change in grain size. BY addition seems to hinder the gain growth. The grain size decreases with increasing BY contents. The grain size of the pure PZT ceramics sintered at 1160 °C is ~7.4 μm, whereas the average grain size abruptly decreases to ~2.5 μm with only 1 mol% of BY. The decrease in grain size becomes more significant with increasing BY content above 2 mol%, showing a grain size of around 1 μm. This can be interpreted as a pinning effect of the secondary phase. Since the microstructure is directly associated with the sintered density, the variation of densities as a function of the content of BY are plotted in Fig. 4. As a result, the PZT–BY(0.01) specimen sintered at 1160 °C shows a maximum value for the sintering density of 7.95 g/cm^3 (99% of theoretical density),

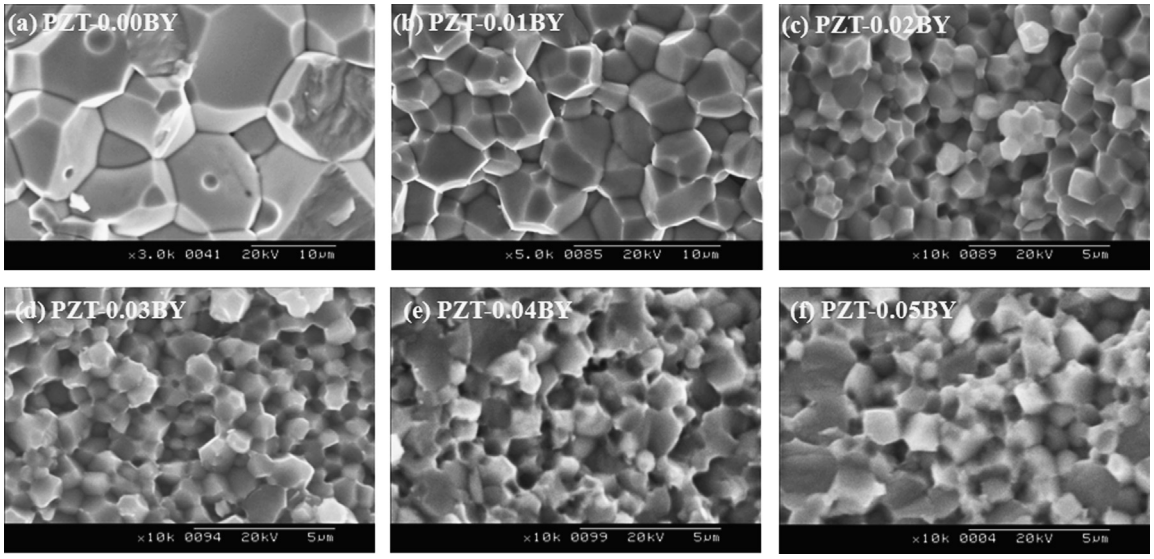

Fig. 3. SEM images of fracture surface of PZT–BY(x) ($0 \le x \le 0.05$) system sintered at 1160 °C for 2 h.

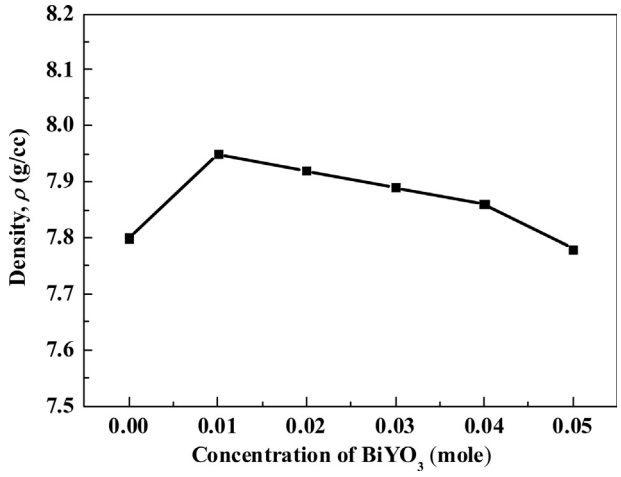

Fig. 4. Density of PZT–BY(x) ceramics sintered at 1160 °C for 2 h with different BY contents.

which then gradually decreases to 7.78 g/cm^3, as the content of BY increases.

Though a secondary phase of BY was not detected at PZT–BY(0.01) as shown in Fig. 2, it is clearly seen that the second phase plays an important role in the reduction of grain size when comparing XRD with SEM results. Considering the fact that the detection limit for identifying a second phase in XRD analysis is about 7 Vol%, the absence of a second phase peak in PZT–BY(0.01) may be attributed to the quite small amount and fine dispersion of the phase. Fig. 3 shows SEM images of the fracture surface for pure and modified PZT–BY ceramics. The pure PZT and PZT–BY(0.01) ceramics indicate a predominantly intergranular fracture [27], while the mixed mode of transgranular and intergranular fracture appears for highly BY-doped ceramics. On the other hand, the intergranular fracture mode of PZT–BY(x) containing $x \ge 0.02$ mol began to change to a mixed mode, as shown in Fig. 3(c)–(f), whereas the mean grain size was decreased. Therefore, the fracture mode transition observed in the PZT–BY(x) seems to be directly related to the content of the secondary phase. As the BY content increases, it can be intuited that the cohesive strength of the grain boundary can be strengthened, possibly due to either by introducing foreign atoms into the relatively weak boundary structure, or by the formation of semi-coherent bonding between the grain interface and precipitates [27].

3.2. *Effects of pre-synthesized $BiYO_3$ doping on the piezoelectric and dielectric properties*

The piezoelectric and dielectric properties of PZT–BY(x) specimens are shown in Fig. 5(a)–(c). The composition containing 0.01 mol of BY [PZT–BY(0.01)] showed the maximum d_{33} and k_p values of 350 pC/N and 65%, respectively, which then decreased as the content of BY increased above 0.02 mol. On the other hand, the behavior of K_{33}^T is inconsistent with the results of piezoelectric properties. K_{33}^T of PZT–BY(0.01) showed the minimum value of 750. The d_{33} and k_p values of pure PZT [PZT–BY(0)] are the lowest at 70 pC/N and 15%, respectively. The values of d_{33} and k_p tend to increase, possibly due to the ease of dipole movement as a consequence of the decrease in the coercive field (E_c) and internal stress with grain coarsening. However, excessive grain coarsening might result in decreasing the overall number of domains. In addition, as can be noticed in the XRD analysis in Fig. 2, phase transition from a tetragonal rich to a rhombohedral rich region appears to occur as the BY content increases, and an MPB forms at 0.01 mol of BY content. As a consequence, the numbers of effective polarization directions were believed to be the maximum at 0.01 mol of BY content [MPB]. With a further increase in the BY content above 0.01 mol, the grain size sharply decreases to ~1 μm, and rhombohedral phase gradually increased with a second phase, accompanying the decrease in d_{33} and k_p. On the other hand, the variation of K_{33}^T differs from those of the piezoelectric properties, as shown in Fig. 5(c). K_{33}^T sharply decreases at

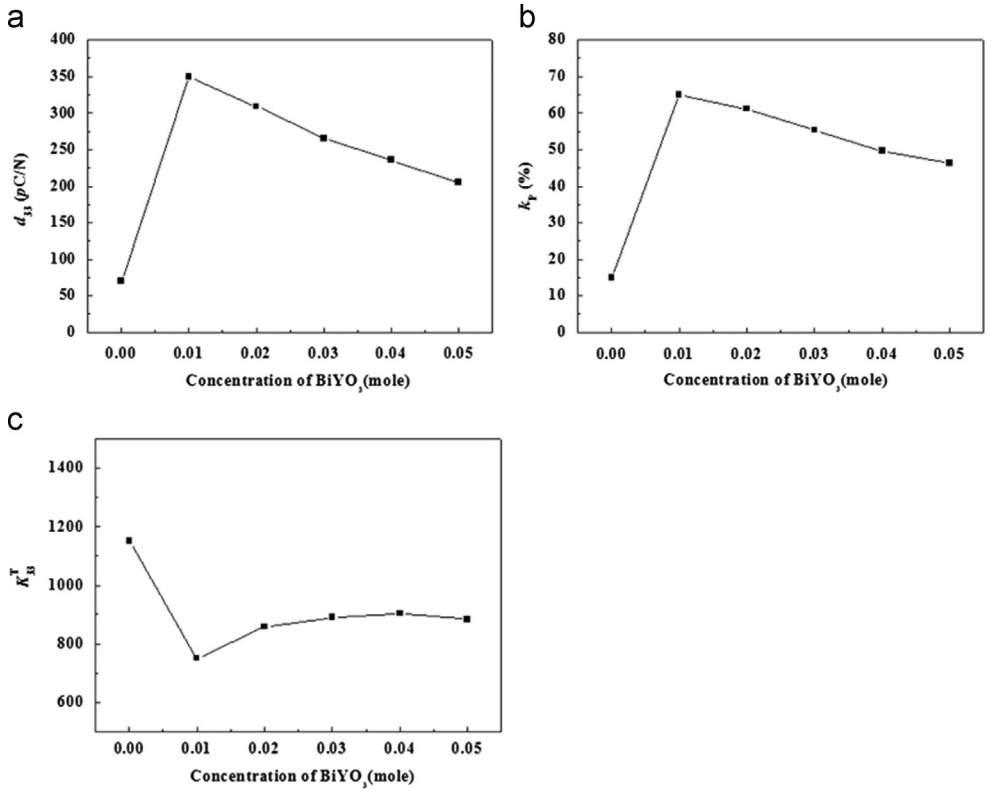

Fig. 5. Variation of piezoelectric and dielectric properties as a function of BY: (a) d_{33}; (b) k_p; and (c) K^T_{33}.

PZT–BY(0.01) as the grain size decreases from ~7.4 μm to 2.5 μm, while it increases slightly with a decreasing grain size of ~1 μm and depends relatively less on the BY content. The increase of K^T_{33} can be interpreted as an effect of the grain size. Okazaki and Nagata [28,29] reported that K^T_{33} at room temperature increases with increasing grain size. They explained this behavior using a space-charge distribution model. According to their model, as the grain size decreases, the grain boundary phase, which is directly related to the volume of space charge regions, increases in size, and finally lowers the dielectric constant of the small-grained PZT. Therefore, K^T_{33} decreases with the PZT–BY(0.01) composition. A further increase in the BY content decreases the grain size to ~1 μm while slightly increasing the dielectric constants. Similarly, Arlt [30] reported that there is a transition region of the domain structure when the grains are small. As the grain size increases over critical values, the structure is changed to a complex banded domain structure, accompanying the relaxation of the internal stress caused by the tetragonal phase, which then increases K^T_{33}. Therefore, a decrease in grain size would be expected to increase the internal stress. This in turn suggests that the dielectric constant increases with decreasing grain size for BY-doped regions.

Fig. 6 shows the temperature dependence of K^T_{33} for the PZT–BY(x) system. Each specimen examined was sintered at 1160 °C. K^T_{33} was almost constant up to 300 °C, and then increased gradually to a maximum value K^T_{33} ($_{max}$) at T_C. Thereafter, K^T_{33} ($_{max}$) decreases with further increases in temperature. This dielectric anomaly indicates a phase transition from ferroelectric to

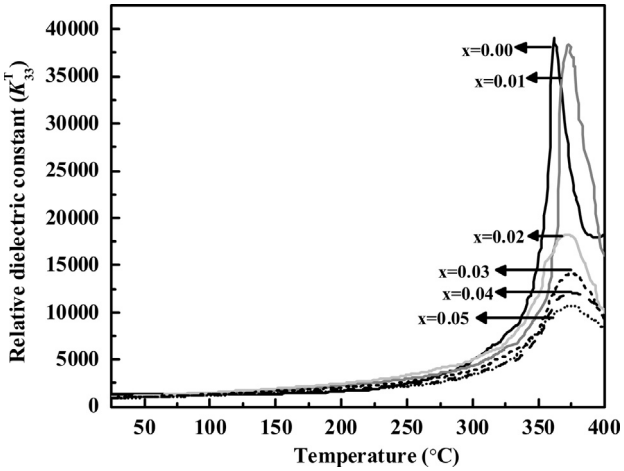

Fig. 6. The temperature dependence of relative dielectric constant for PZT–BY (x) system sintered at 1160 °C for 2 h.

paraelectric phase at T_C. The T_C of pure PZT is ~360 °C. Upon adding 0.01 mol of BY, T_C shifted towards a higher temperature (T_C ~373 °C). Further shift is not found in T_C, but peak broadening occurred, as shown in Fig. 6. It is evident that the value of K^T_{33} ($_{max}$) sharply decreases as the content of BY increases to 0.02 mol, and the dielectric peak broadened rather than sharpening around T_C, which is one of the characteristics of disordered perovskite structure with diffuse phase transition. This broadening is believed to be due to the compositional fluctuation [31] leading to a microscopic heterogeneity in composition, and thus, to a distribution of different local T_C, caused by the appearance of a second

phase [BY]. It is well known that cubic phase addition to PZT reduces T_C, but in the PZT system with BY added, T_C increased. This result can be explained in terms of internal stress, which retards the ferroelectric and paraelectric transition. The internal stress increases with a decrease of grain size. Internal stress in ferroelectric grains can be accumulated by the pinning effect of the secondary phase, and the increase in the internal stress can be effectively reduced by the formation of a twin-like 90° domain, which increases the stability of the ferroelectric state [32,33]. Therefore, the transition temperature can be suppressed by BY doping.

Further evidence for the BY doping and grain size effect are obtained by examining the polarization–electric field (*P–E*) curve at room temperature. The variation of the hysteresis loops of P_r and E_c for pure and BY-doped PZT samples sintered at 1160 °C is shown in Fig. 7(a) and (b). The values of P_r and E_c are determined from the measured loops. In the data of hysteresis loops, P_r for the PZT–BY(0.01) specimen has the highest value of 50 μC/cm^2. Therefore, the increase of the piezoelectric properties is closely related to the increase of P_r, whereas E_c sharply increases and has a similar values as the BY content increases above 0.02 mol and the grain size decreases around ~1 μm. Therefore, these results are in agreement with a previous analysis of the piezoelectric/dielectric properties as a clamping effect caused by internal stress below a critical grain size with a second phase.

To investigate the effects of the BY doping method on the microstructure and electrical properties, the SEM morphology of the pre-synthesized and conventionally mixed PZT–BY (0.01) samples sintered at the same temperature is shown in Fig. 8(a) and (b). The conventionally mixed sample has a larger average grain size of ~4.9 μm with irregular grain shape compared with that of ~2.5 μm in the pre-synthesized sample. In addition, the electrical properties of PZT–BY(0.01) samples sintered at the same temperature have been listed in Table 1. The piezoelectric properties of the pre-synthesized PZT–BY (0.01) specimen show higher values than those of the PZT–BY (0.01) specimen fabricated by the conventional mixed-oxide method. The observed increase of the piezoelectric properties can be interpreted as the effects of the higher density and the decrease of grain size caused by the pinning effect of pre-synthesized BY.

Similarly, Haertling and Zimmer [34] reported that the piezoelectric properties increased with decreasing porosity of the PZT ceramics. Therefore, it can be concluded that the pre-synthesis process increases the sintering density and decreases the porosity, which in turn accompanies the increase of the piezoelectric properties. Since the dielectric properties are directly associated with grain size, the conventional mixed sample has a larger average grain size and shows a higher value than that of the pre-synthesized sample. From considerations of the ionic radii, it is highly probable that Bi and Y ions occupy the Pb sites and form Pb vacancies in the case of the conventional mixed sample, accompanying the donor doping effect, hence favoring an increase of the piezoelectric

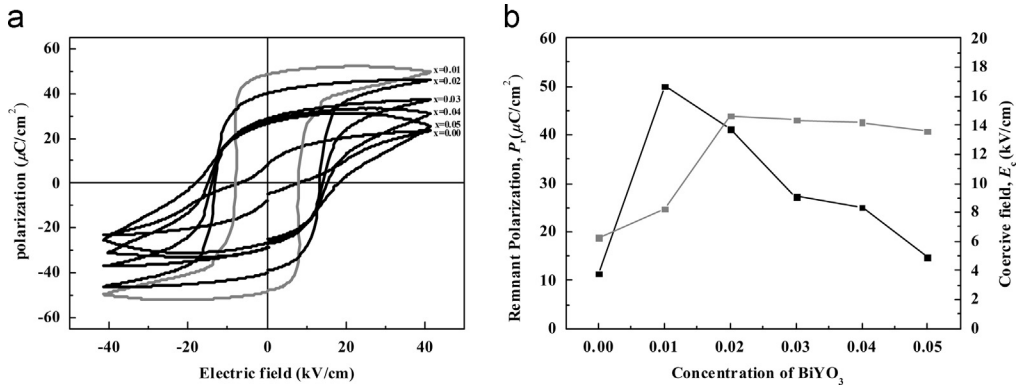

Fig. 7. (a) Room temperature *P–E* hysteresis of PZT–BY(*x*) ternary ceramics sintered at 1160 °C and (b) P_r and E_c measured from their corresponding hysteresis loops.

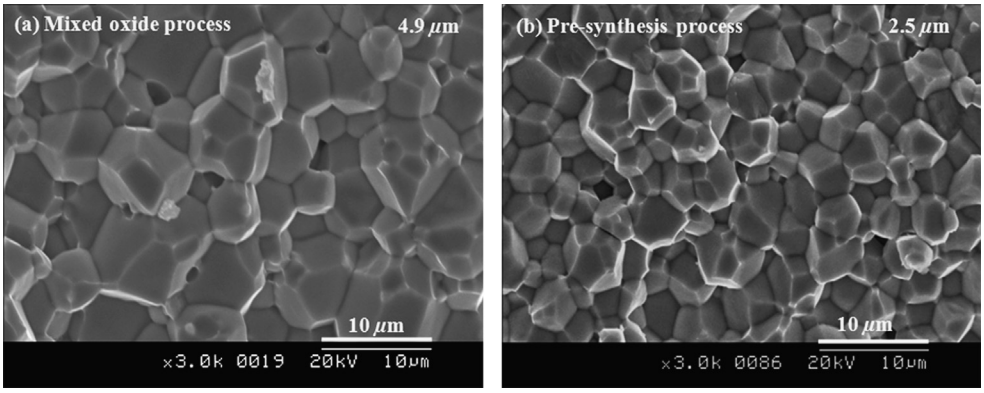

Fig. 8. SEM images of fracture surface of PZT–BY(0.01) prepared by (a) mixed oxide process and (b) pre-synthesized process.

Table 1
The comparative parameters of PZT–BY(0.01) obtained with mixed oxide route and pre-synthesized process sintered at 1160 °C for 2 h.

Properties	Mixed route	Pre-synthesis
Density (%)	97	99
d_{33} (pC/N)	278	350
k_p (%)	56	65
K_{33}^T	820	750

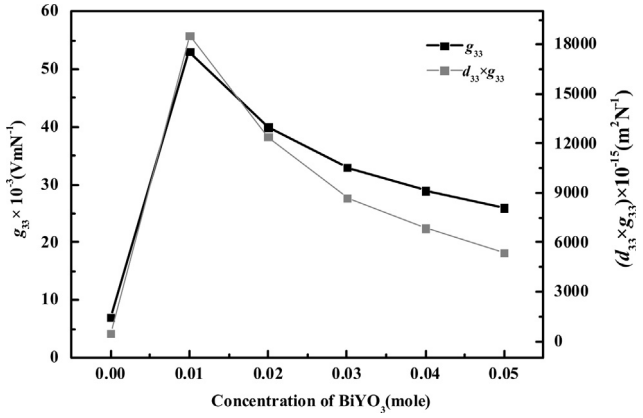

Fig. 9. Variations of the g_{33} and $(d_{33} \times g_{33})$ values of PZT–BY(x) ceramics fabricated by pre-synthesis process.

properties compared to pure PZT. Pre-synthesized BY may precipitate at the grain boundary as a secondary phase and compensate for the vacancies in the vicinity of PZT grains, where defects can accumulate. Therefore, pre-synthesized BY seems to play an important role in the pinning and doping effect, simultaneously. In view of these facts, one can conclude that pre-synthesized BY enhances the piezoelectric properties and reduces the grain size, and is more favorable than the conventional mixed-oxide method.

Variations of the g_{33} and $(d_{33} \times g_{33})$ values are illustrated in Fig. 9. The calculated data of g_{33} and $(d_{33} \times g_{33})$ for PZT–BY (x) has been shown in the Table 2. A maximum g_{33} of 53.0×10^{-3} Vm/N and $(d_{33} \times g_{33})$ of $18{,}549 \times 10^{-15}$ m^2/N were obtained for PZT–BY(0.01) fabricated by pre-synthesized process. This value is comparable to the highest value reported so far for polycrystalline ceramics [8,11,12,17]. The increase in the g_{33} and $(d_{33} \times g_{33})$ values was related to the decreased K_{33}^T, while a high d_{33} value was maintained at x=0.01. On the other hand, the g_{33} and $(d_{33} \times g_{33})$ values decreased for $x \geq 0.02$ mol, because of the decrease in the d_{33} value and increasing behaviors of the K_{33}^T. These results were in agreement with the previous analysis of the piezoelectric properties (Fig. 5). In order to identify figure of merit in a transverse vibration mode, the g_{31} and $(d_{31} \times g_{31})$ values are also obtained and summarized for PZT–BY(0.01) as shown in Table 3.Typical values for energy harvesting piezoelectric materials are shown in Table 4 obtained from selected references. Most of the recent work reported a high transduction coefficient in the various relaxor materials doped PZT system. The doped relaxor materials generally enhanced the

Table 2
Calculated values of g_{33} and $(d_{33} \times g_{33})$ at different moles of BY addition in PZT fabricated by pre-synthesis process.

BY (mole)	$g_{33} \times 10^{-3}$(Vm/N)	$(d_{33} \times g_{33}) \times 10^{-15}$ (m^2/N)
0.00	7	478
0.01	53	18549
0.02	40	12399
0.03	33	8692
0.04	29	6882
0.05	26	5376

Table 3
Longitudinal and transverse piezoelectric coefficients and their corresponding figure of merits.

Longitudinal mode		Transverse mode	
d_{33} (pC/N)	350	d31 (pC/N)	−181
$g_{33} \times 10^{-3}$ (Vm/N)	53	g31 × 10−3 (Vm/N)	−27.39
$(d_{33} \times g_{33}) \times 10^{-15}$ (m^2/N)	18549	(d31 × g31) × 10−15 (m2/N)	−4957

piezoelectric coefficients, while it abruptly lowered T_c [35]. Thus, low T_c limits the application fields of these materials. On the other hand, BY-doped PZT showed a transduction coefficient without lowering T_c (~373 °C). In view of these facts, one can consider that the PZT–BY system may be suitable composition that does not have a lower T_c. The PZT–BY(0.01) composition could be very useful for specific applications in piezoelectric, ultrasonic, and energy harvesting devices.

4. Conclusion

A new-ternary solid solution of PZT–BY(x) ($0 \leq x \leq 0.05$) was systematically investigated. Second phases were found to precipitate in the composition containing $x \geq 0.01$ mol of BY. A denser and finer microstructure was observed for BY-doped PZT compared to undoped PZT. The optimal doping level was found to be $x = 0.01$, which yielded a K_{33}^T of 750, T_C of 373 °C, P_r of 50 μC/cm^2, d_{33} of 350 pC/N, and k_p of 65%.The present study has revealed that a high d_{33} and k_p with a low K_{33}^T value could be achieved by the pre-synthesis fabrication process. With the observed enhanced electromechanical parameters, a maximum g_{33} of 53.0×10^{-3} Vm/N and $(d_{33} \times g_{33})$ of $18{,}549 \times 10^{-15}$ m^2/N were obtained with PZT–BY(0.01). The attained piezoelectric characteristics with a high level of g_{33} and high figure of merit offer ample opportunity for using this ceramic as a base in energy harvesting devices.

Acknowledgments

This research was supported by the Regional Innovation Center (RIC) Program conducted by the Ministry of Knowledge Economy of the Korean Government.

Table 4
Properties of some PZT-based energy harvesting materials.

Composition	$g_{33} \times 10^{-3}$ (Vm/N)	$d_{33} \times g_{33}(10^{-15}$ m^2/N)	T_c (°C)	Ref. no.
$Pb(Zr_{1-x}Ti_x)O_3$–$Pb(Ni_{1/3}Nb_{2/3})O_3$	33.3	15853		11
$(1-x)Pb(Zr_{0.47}Ti_{0.53})O_3$–$xPb[(Ni_{0.6}Zn_{0.4})_{1/3}Nb_{2/3}]O_3$	31	19572		17
$(0.65+y)Pb(Zr_{0.47}Ti_{0.53})$–$(0.35-y)Pb[(Ni_{1-x}Zn_x)_{1/3}Nb_{2/3}]O_3$	36	20056		18
$Pb_{1-z}La_z(NiSb)_{0.05}[(Zr_{0.52}$–$Ti0.48)_{1-Z/4}]_{0.95}O_3$	39.3	16200		19
$0.99Pb(Zr_{0.53}Ti_{0.47})O_3$–$0.01BiYO_3$	53	18549	373	present

References

[1] W.J. Choi, Y. Jeon, J.-H. Jeong, R. Sood, S.-G. Kim, Energy harvesting MEMS device based on thin film piezoelectric cantilevers, Journal of Electroceramics 17 (2006) 543–548.

[2] P. Muralt, M. Marzencki, B. Belgacem, F. Calame, S. Basrour, Vibration Energy Harvesting with PZT Thin Film Micro Device, PowerMEMS, Washington DC, USA407–410.

[3] P.D. Mitcheson, E.M. Yeatman, G.K. Rao, A.S. Holmes, T.C. Green, Energy harvesting from human and machine motion for wireless electronic devices, Proceedings of the IEEE 96 (9) (2008) 1457–1486.

[4] H. Miyabuchi, T. Yoshimura, N. Fujimura, S. Murakami, Direct piezoelectricity of PZT films and application to vibration energy harvesting, Journal of the Korean Physical Society 59 (3) (2011) 2524–2527.

[5] H. Liu, C. Quan, C.J. Tay, T. Kobayashi, C. Lee, A MEMS-based piezoelectric cantilever patterned with PZT thin film array for harvesting energy from low frequency vibrations, Physics Procedia 19 (2011) 129–133.

[6] S. Tadigadapa, K. Mateti, Piezoelectric MEMS sensors: state-of-the-art and perspectives, Measurement Science and Technology 20 (9) (2009) 092001-1–092001-30.

[7] T. Harigai, H. Adachi, E. Fujii, Vibration energy harvesting using highly (001)-oriented Pb (Zr, Ti)O_3 thin film, Journal of Applied Physics 107 (2010) 096101.

[8] J.H. Cho, R.F. Richards, D.F. Bahr, C.D. Richards, M.J. Anderson, Efficiency of energy conversion by piezoelectrics, Applied Physics Letters 89 (2006) 104107.

[9] Z. Wang, Y. Xu, Vibration energy harvesting device based on air-spaced piezoelectric cantilevers, Applied Physics Letters 90 (2007) 263512.

[10] M. Ferrari, V. Ferrari, M. Guizzetti, D. Marioli, A. Taroni, Piezoelectric multi frequency energy converter for power harvesting in autonomous micro systems, Sensors and Actuators A 142 (2008) 329–335.

[11] I.-T. Seo, C.-H. Choi, I.-Y. Kang, S. Nahm, S.B. Kim, D. Song, J. Lee T.H. Sung, J.-H. Paik, The high energy density of $Pb(Zr_{1-x}Ti_x)O_3$–$Pb(Ni_{1/3}Nb_{2/3})O_3$ ceramics for piezoelectric energy harvesting devices, Journal of Ceramic Processing Research 13 (6) (2012) 739–743.

[12] C. Green, K.M. Mossi, R.G. Bryant, In scavenging energy from piezoelectric materials for wireless sensor applications, Proceedings of ASME International Mechanical Engineering Congress and R&D Expo (2005).

[13] A. Mathers, K.S. Moon, Y.A. Jingang, Vibration-based PMN-PT energy harvester, IEEE Sensors Journal 9 (2009) 731–739.

[14] A. Islam, S. Priya, High energy density composition in the system PZT-PZNN, Journal of the American Ceramic Society 89 (2006) 3147–3156.

[15] H.W. Kim, S. Priya, K. Unchino, R. Newnham, Piezoelectric energy harvesting under high pre-stressed cyclic vibrations, Journal of Electroceramics 15 (2005) 27–34.

[16] A.J. Moulson, J.M. Herbert, Electrocramics: Materials, Properties, Application, second ed, Wiley & Sons, England384.

[17] Y.J. Cha, I.T. Seo, I.Y. Kang, S.B. Shin, J.H. Choi, S. Nahm T.H. Seung, J.H. Paik, Effect of the structural properties on the energy density of $Pb(Zr_{0.47}Ti_{0.53})O_3$–$Pb[(Ni_{0.6}Zn_{0.4})_{1/3}Nb_{2/3}]O_3$ ceramics, Journal of Applied Physics 110 (2011) 084111-1-6.

[18] I.T. Seo, Y.J. Cha, I.Y. Kang, J.H. Choi, S. Nahm, T.H. Seung, J.H. Paik, High energy density piezoelectric ceramics for energy harvesting devices, Journal of the American Ceramic Society 94 (2011) 3629–3631.

[19] C.M. Lonkar, D.K. Kharat, H.H. Kumar, S. Prasad, K. Balasubramanian, Effect of La on piezoelectric properties of $Pb(Ni_{1/3}Sb_{2/3})O_3$–$Pb(ZrTi)O_3$ ferroelectric ceramics, Journal of Materials Science: Materials in Electronics 24 (2013) 411–417.

[20] S.-J. Yoon, J.H. Moon, H.-J. Kim, Piezoelectric and mechanical properties of Pb $(Zr_{0.52}Ti_{0.48})$ O_3–$Pb(Y_{2/3}W_{1/3})O_3$ ceramics, Journal of Materials Science 32 (3) (1997) 779–782.

[21] W. Qiu, H.H. Hng, Effects of addition of $Pb(Y_{1/2}Nb_{1/2})O_3$ on microstructure and piezoelectric properties of $Pb(Zr_{0.53}Ti_{0.47})O_3$, Ceramics International 30 (2004) 2171–2176.

[22] G.H. Haertling, Grain growth and densification of hot-pressed lead zirconate–lead titanate ceramics containing bismuth, Journal of the American Ceramic Society 49 (3) (1966) 113.

[23] J.S. Cross, S.-H. Kim, S. Wada, A. Chatterjee, Characterization of Bi and Fe co-doped PZT capacitors for FeRAM, Science and Technology of Advanced Materials 11 (2010) 044402.

[24] K.B. Lee, H.S. Lee, Characterization of a bismuth-doped lead zirconate titanate thin film capacitor, Journal of the Korean Physical Society 31 (3) (1997) 532–536.

[25] K.L. Yadav, Structural, dielectric and ferroelectric properties of Y^{3+} doped PZT (65/35), Advanced Materials Letters 1 (3) (2010) 259–263.

[26] IRE standards on piezoelectric crystals: measurements of piezoelectric ceramics, in: Proceedings of the Institute of Radio Engineers, 49 (7) (1961) 1161–1169.

[27] R.-F. Yue, W.-Z. He, F.-F. An, J. Yu, G.-C. Chen, Preparation of PZT-based piezoceramics with transgranular fracture mode, Ceramics International 38S (2012) S225–S228.

[28] K. Okazaki, K. Nagata, Mechanical behaviour of materials, Journal of the Society of Materials Science (Japan) 4 (1972) 404.

[29] K. Okazaki, K. Nagata, Effects of grain size and porosity on electrical and optical properties of PLZT ceramics, Journal of the American Ceramic Society 56 (1973) 83.

[30] G. Arlt, The influence of microstructure on the properties of ferroelectric ceramics, Ferroelectrics 104 (1990) 217–227.

[31] A. Chamola, H. Singh, U.C. Naithani, Study of $Pb(Zr_{0.65}Ti_{0.35})O_3$ doping on structural, dielectric and conductivity properties of $BaTiO_3$ ceramics, Advanced Materials Letters 2 (2) (2011) 148–152.

[32] K. Uchino, Piezoelectric Actuators and Ultrasonic Motors, Kluwer Academic Publishers, USA, 1997.

[33] W.R. Bussem, L.E. Cross, A.K. Goswami, Phenomenological theory of high permittivity in fine grained barium titanate, Journal of the American Ceramic Society 49 (1) (1966) 33–36.

[34] G.H. Haertling, W.J. Zimmer, Analysis of hot pressing parameters for lead–zirconate–lead titanate ceramics containing two atom percent bismuth, American Ceramic Society Bulletin 45 (1966) 1084–1089.

[35] S. Wagner, D. Kahraman, H. Kungl, M.J. Hoffmann, C. Schuh, K. Lubitz, H. M.-Biesenecker, J.A. Schmid, Effect of temperature on grain size, phase composition, and electrical properties in the relaxor-ferroelectric-system $Pb(Ni_{1/3}Nb_{2/3})O_3$–$Pb(Zr,Ti)O_3$, Journal of Applied Physics 98 (2005) 024102.